# Implementation of an Adaptive Balancing Hybrid

BERTON E. DOTTER, JR., ALEJANDRO DE LA PLAZA, DAVID A. HODGES, FELLOW, IEEE, AND DAVID G. MESSERSCHMITT, SENIOR MEMBER, IEEE

*Abstract*—**Two implementations of an adaptive balancing hybrid are described. The first is predominly analog, in which the adaptation parameter $\theta$ is a continuous analog quantity, while the second is predominly digital, in which $\theta$ has a two-bit representation. Experimental results are reported.**

## I. INTRODUCTION

IN [1] an adaptive balancing hybrid was described for application to the two-wire to four-wire interface of a local digital switch. This adaptive hybrid automatically selects the appropriate balance network for loaded and nonloaded subscriber loops, using as the basis for adaptation speech or other signals present on the receive four-wire path.

In this paper we describe two different implementations of an adaptive balancing hybrid based on the basic principle described in [1]. One is a completely analog realization, in which the single adaptation parameter $\theta$ is allowed to assume any value between zero and one. The second is a partially digital realization in which $\theta$ is allowed to assume one of four values, and hence, can be represented as a 2-bit binary number.

The analog hybrid can achieve a slightly better balance since it has available a continuum of $\theta$, but four values of $\theta$ are adequate to achieve singing margin objectives. In fact, just two values of $\theta$, $\theta = 0$ and $\theta = 1$, yield an acceptable singing margin distribution. The same principles used in the design of the 2-bit digital realization can be used to achieve any number of bits of precision. The primary advantage of the digital realization is the capability to store the appropriate value of $\theta$ indefinitely, as between calls, avoiding the need to readapt at the beginning of each call.

Laboratory experience with these two hybrids will be related. Both hybrids were tested under ideal laboratory conditions using artificial subscriber lines and using as test signals tones, random noise, and speech. Neither hybrid has been tested in a field environment with actual subscriber loops, which would presumably be a requisite to widespread use.

In Section II we describe the basic configuration common to both realizations, and in Sections III and IV we describe both the implementation and experimental results for the analog and digital realizations, respectively.

Paper approved by the Editor-in-Chief of the IEEE Communications Society for publication after presentation at the 1980 International Conference on Communications, Seattle, WA, June, 1980. Manuscript received January 4, 1980; revised March 12, 1980. This work was supported in part by a grant to the University of California from TRW VIDAR. Portions of this work were submitted by A. de la Plaza to the University of California in partial fulfillment of the Master of Science degree.

B. E. Dotter and A. de la Plaza are with TRW VIDAR, Mountain View, CA 94040.

D. A. Hodges and D. G. Messerschmitt are with the Department of Electrical Engineering and Computer Sciences and the Electronics Research Laboratory, University of California, Berkeley, CA 94720.

## II. BASIC CONFIGURATION

The same basic configuration for the adaptive balancing hybrid shown in Figs. 1 and 2 applies to both the analog and digital realizations.

The basic electronic hybrid with controlled balance is shown in Fig. 1. The gain $K_1$, approximately 9 dB, compensates for the hybrid losses and transformer losses in order to provide 0 dB 900 Ω insertion loss from two-wire to two-wire port. Two terminations $Z_1$ and $Z_2$ provide a compromise balance for loaded and nonloaded subscriber loops, respectively. The resistance $R$ is the input impedance of the hybrid, chosen to be 900 Ω. The two-wire port has, in addition to the near-end talker (NET), a component of the far-end talker (FET) which is partially cancelled by subtracting $\hat{x}(t)$ in a differential amplifier to yield the transmit signal $z(t)$. The parameter $\theta$ is used to control the relative weighting of the two terminations. Finally, the signal $w(t)$ is used in later adaptation circuitry to control $\theta$.

A block diagram of the total adaptive balancing hybrid is shown in Fig. 2. The controlled balance hybrid of Fig. 1 is connected to transmit and receive analog four-wire ports of the switch and via its two-wire port to the subscriber loop using a transformer for balanced-to-unbalanced conversion, isolation, and battery feed.[1] An adaptation control circuit uses $w(t)$ and $z(t)$ to generate the adaptation parameter $\theta$, and adaptation is disabled in the presence of a detectable NET by a NET detector.

The adaptation control and NET detector differ for the two implementations, and will be described in Sections III and IV along with experimental results.

## III. ANALOG IMPLEMENTATION

Due to the fact that $0 \leqslant \theta \leqslant 1$, the linear combination of $r_1(t)$ and $r_2(t)$ in the controlled-balance hybrid of Fig. 1 can be performed without multipliers by the variable duty-cycle switch of Fig. 3. The duty cycle, which is $\theta$, was generated by comparing a sawtooth wave to $\theta$. The sawtooth fundamental frequency was chosen to be 50 kHz, much higher than the signal frequencies of interest. It is easily shown that the output spectrum is the desired weighted combination $\theta r_1(t) + (1 - \theta) r_2(t)$ plus aliased spectra centered at multiples of 50 kHz, the switching rate.

$Z_1$ and $Z_2$ in Fig. 1 were parallel $RC$ circuits designed for loaded and nonloaded cables, and were slightly modified to compensate for the nonideal transformer. This was done by adding a series resistor to each parallel $RC$ combination, equal to the total series resistance of the transformer windings, and

[1] The technique for adaptive balance described here could be used equally well with other transformerless means of interfacing a subscriber loop.

0090-6778/80/0800-1408$00.75 

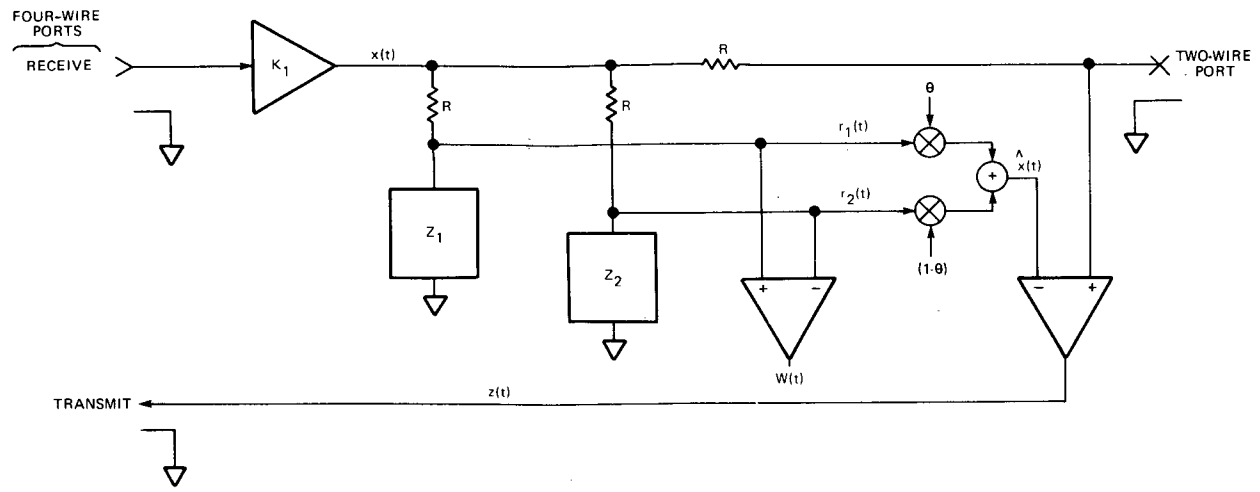


Fig. 1. Controlled-balance electronic hybrid.

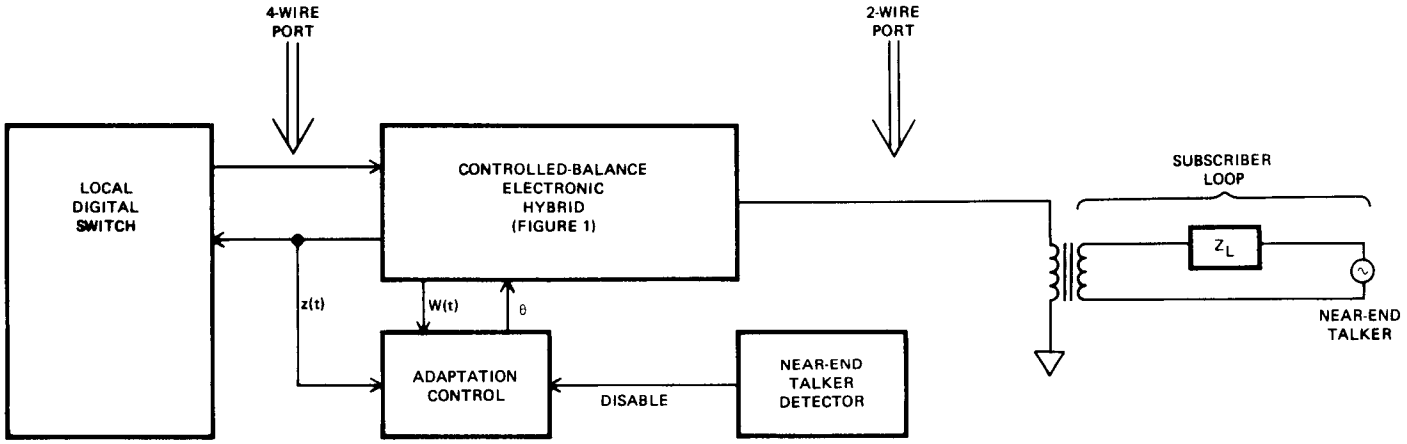


Fig. 2. Block diagram of adaptive balancing hybrid.

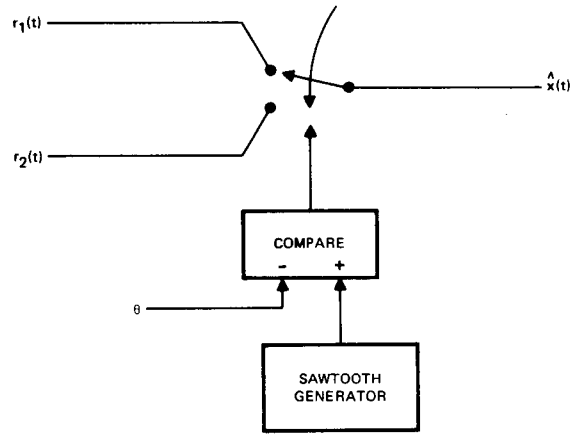


Fig. 3. Generation of $x(t)$ in analog implementation.

shunting the transformer output with a small capacitor to compensate for the magnetizing inductance.

The adaptation control (Fig. 4) cross correlates sgn $w(t)$ with $z(t)$ by switching $z(t)$ or $-z(t)$ to the input of an integrator depending on the sign of $w(t)$, as recommended in [1]. Adaptation can be disabled by grounding the integrator input, in which case the old $\theta$ is retained until the capacitor is discharged by offset currents.

The NET detector was designed to have

1) Fast attack time to take full advantage of the presence of a FET;
2) Slow decay time to allow any echo from a NET to decay sufficiently;
3) A threshold of operation to suppress adaptation on low-level noise signals; and
4) Virtually instantaneous disabling of adaptation upon detection of a NET.

The NET detector is shown in Fig. 5. Transmit signal $z(t)$ is full-wave rectified and fed through a passive low-pass filter with transfer function $1 + 1/(sa + 1)$, and a dc bias voltage is added. A dc bias of 0.65 V and an $RC$ time constant of 0.87 ms were used. The low-pass filter provided fast attack and slow decay times and the dc bias provided the constant threshold. The output, labeled as $m(t)$, contains primarily near-end energy, and is compared with $K_2 \mid w(t) \mid$, which contains only far-end energy. The comparator output enables the switch in Fig. 4, and controls whether or not the integrator input is grounded.

This talker detector is very simple and hence imperfect in its operation. However, since the subscriber line impedance is not expected to vary significantly with time (extension phones, for example, should not change the optimum $\theta$ significantly), very slow adaptation is permissible, particularly if $\theta$ is retained

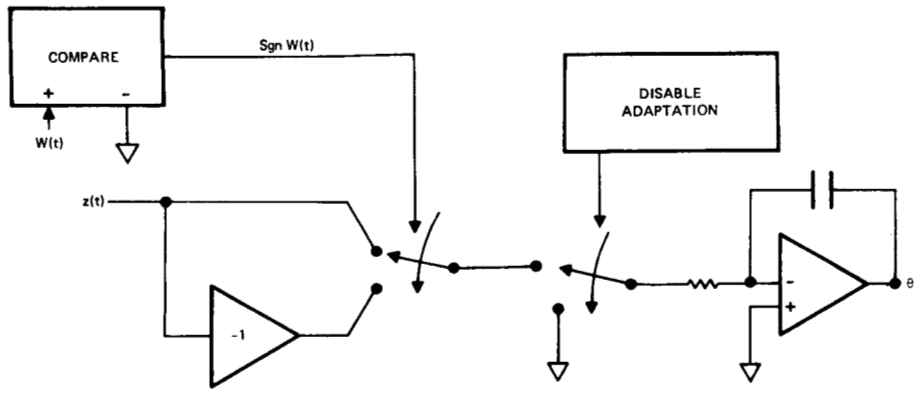


Fig. 4. Adaptation control in analog implementation.

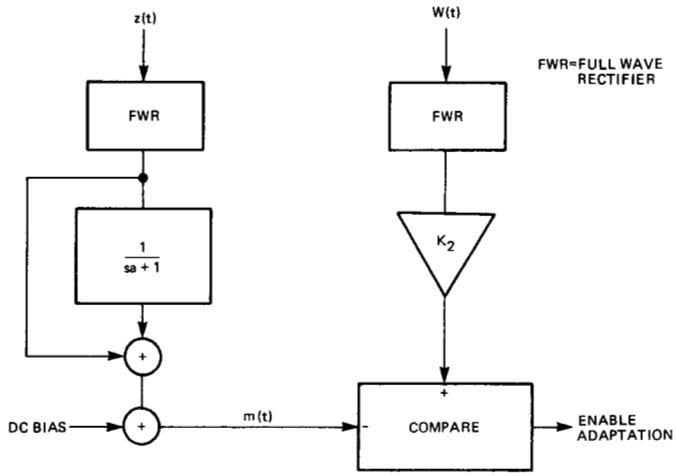


Fig. 5. NET detector in analog implementation.

from call to call. Slow adaptation (small integration constant) can compensate to a large degree for imperfect NET detection, since the long-term fraction of time for which double-talking exists is expected to be small. Slow adaptation also reduces the variation of $\theta$ after convergence [1].

Two breadboard adaptive hybrids were built and placed back-to-back with a *D*-type channel bank in the four-wire path to simulate the effect of low-pass filtering and delay (about 800 $\mu$s for a *D*-bank). The two-wire ports were connected to artificial lines terminated with 500 telephone sets or other signal sources, including a sinusoidal oscillator, two radios tuned to two different radio talk stations (no noise added), and a noise generator. The noise generator could produce an echo return loss (ERL) spectrum in the band 500 to 2500 Hz, and a singing return loss (SRL) spectrum from 200 to 500 Hz (SRL-LO) or 2500 to 3200 Hz (SRL-HI) [2, pp. 492-494]. The 900 $\Omega$ insertion loss between two-wire ports was adjusted to 0 dB. For this implementation, adaptation rate was set so that adaptation was completely reliable and there was no appreciable variation in $\theta$ after convergence for even very severe double-talking (two independent nonconversational talkers using two radio talk stations). For this case adaptation time would sometimes approach 2 min, whereas for a single talker it was consistently less than 1 min. Fig. 6 shows strip-chart recordings of $\theta$ adapting for several cases. For conversational speech with less double-talking and greater $\theta$ variation, the adaptation rate could presumably be speeded up considerably (for example, in the implementation of Section IV the adaptation time is about 2 s).

The analog implementation has a continuous range of $\theta$ available, and experiments have shown that the optimum $\theta$ is clearly a function not only of whether the cable is loaded or nonloaded but also cable length and FET spectrum. Fig. 7 shows optimum $\theta$ versus cable length for the several noise spectra. Notice that for several cases the optimum $\theta$ is some intermediate value between 0 and 1. This has also been confirmed by computer analysis. This implies that a better balance is obtained for these cases than would be obtained by either of the two terminations individually.

Of particular concern with an adaptive hybrid is the problem of singing, namely, whether singing can ever occur and whether, if it does, the hybrid can adapt out of that state. In fact, under the described experimental conditions initial singing was never observed, even under extreme conditions such as short-circuited or open-circuited two-wire ports. When 2 dB of insertion gain was inserted singing could be induced, but surprisingly the hybrid was able to adapt on the basis of the singing signal, to the point where the singing power was below the threshold where adaptation was disabled. Any significant talker power was then able to complete the adaptation, removing the singing condition entirely.

## IV. DIGITAL IMPLEMENTATION

This implementation differs from the analog implementation primarily in the fact that one of a finite number of values of $\theta$ is stored in an up-down counter. As a result, when adaptation is disabled (as between calls) $\theta$ can be retained indefinitely. In addition, this implementation includes several other innovations, including an insensitivity of adaptation speed to signal power, as well as the NET detector described in [1].

In the digital implementation, $\theta$ was stored as a 2-bit word, and the four values of $\theta$ were achieved by a multiplying digital-to-analog converter (MDAC) as shown in Fig. 8. The output voltage is, as desired

$$v_0 = \theta r_1(t) + (1 - \theta) r_2(t)$$

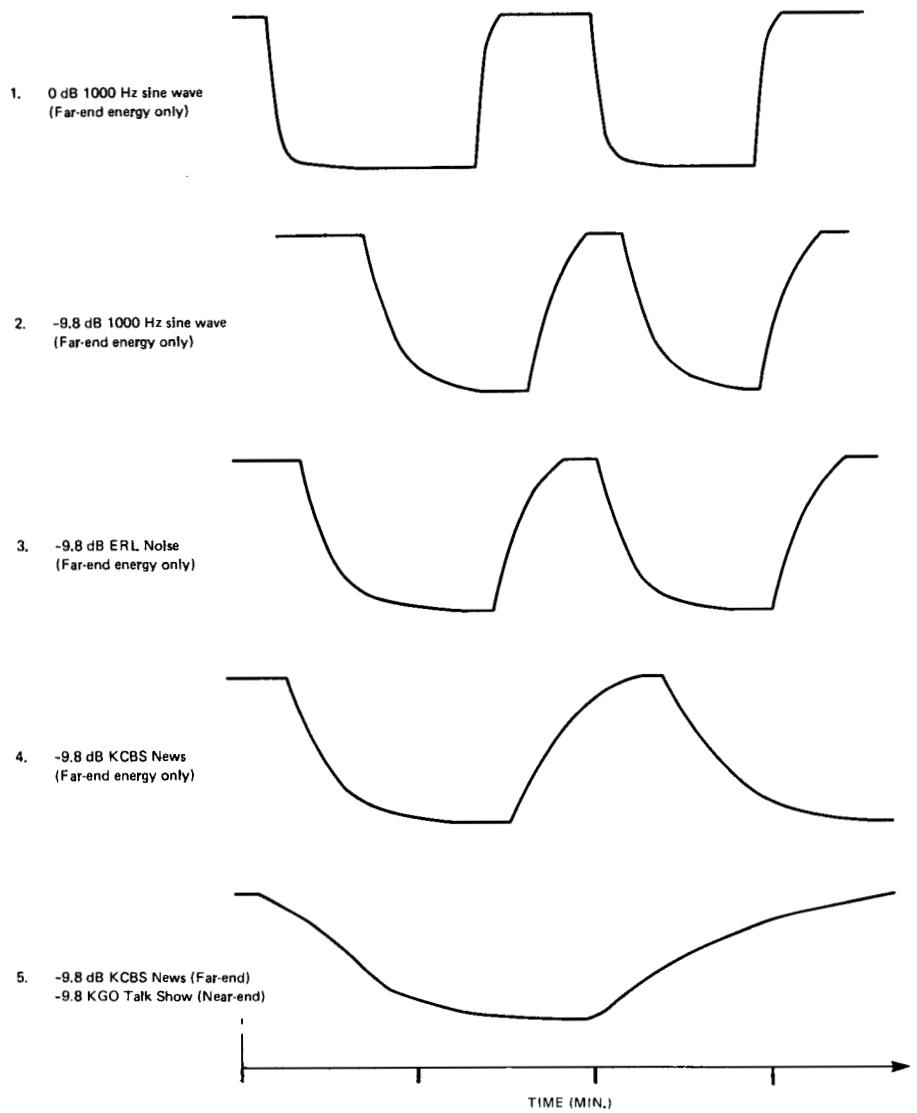


Fig. 6. $\theta$ versus time in analog implementation.

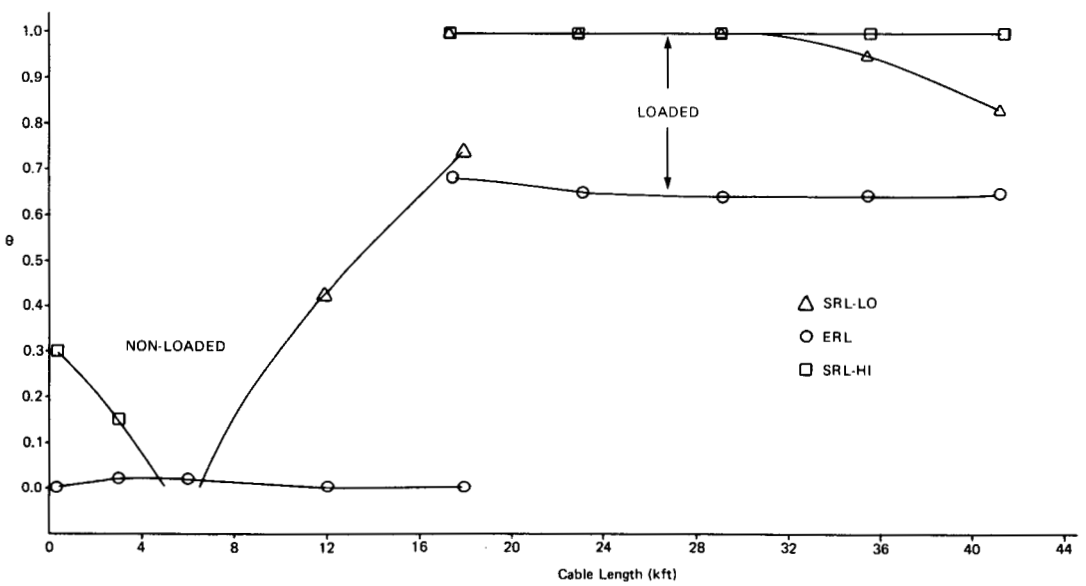


Fig. 7. Dependence of $\theta$ on cable length and FET spectrum.

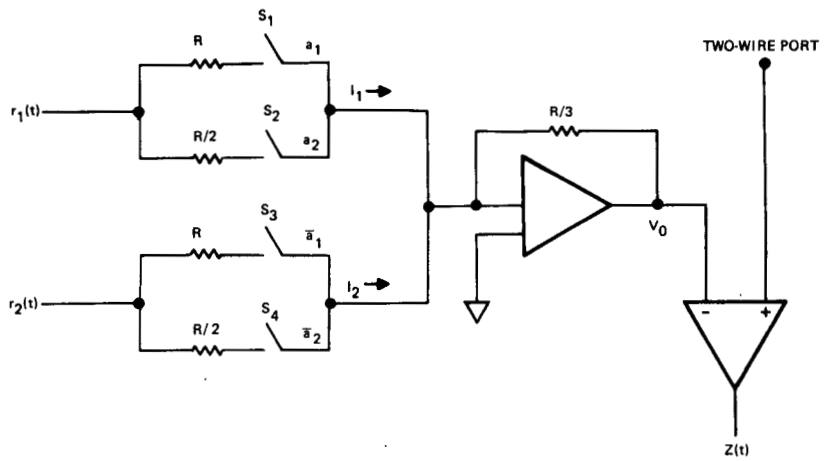


Fig. 8. Controlled hybrid in digital implementation.

where

$$\theta = \tfrac{1}{3}(2a_2 + a_1)$$

$$(1-\theta) = \tfrac{1}{3}(2\bar{a}_2 + \bar{a}_1)$$

and $a_1$ and $a_2$ represent the state of switches $S_1$ and $S_2$ ($a_1 = 1$ if $S_1$ is closed and $a_1 = 0$ if it is open).

The adaptation control is shown in Fig. 9. The factor $\theta$ is stored in an up-down counter, which can count up or down at each positive zero-crossing of $w(t)$ if either the up or down input is high. Overflow and underflow are prevented by disabling the clock by simple logic whenever the counter contains (11) or (00) and the up or down input is enabled.

The basic problem, then, is to determine when it is appropriate to count up or down. As shown in [1], when $z(t)$ and $w(t)$ are Gaussian,

$$E[z(t)\ \text{sgn}\ w(t)] = \sqrt{\frac{2}{\pi}}\,\sigma_w(\theta_0 - \theta)$$

where $E$ is expectation, $\sigma_w$ is the standard deviation of $w(t)$, and $\theta_0$ is the optimum value of $\theta$. In Fig. 9, the product $z(t)$ sgn $w(t)$ is formed in the same manner as in the analog implementation, and it is filtered by a single-pole low-pass filter to form an estimate $u_1$ of the expectation. In order to interpret the size of $u_1$, a second signal $u_2$, which is an estimate of

$$E[w(t)\ \text{sgn}\ w(t)] = \sqrt{\frac{2}{\pi}}\,\sigma_w$$

is also formed. It is appropriate to count up when

$$\theta_0 - \theta > \xi \quad \text{or}\ u_1 > \xi u_2$$

where $\xi$ is a threshold; count down when

$$\theta_0 - \theta < \xi \quad \text{or}\ u_1 < \xi u_2$$

and otherwise retain the same $\theta$. The size of $\xi$ can readily be determined. In general if there are $2^N$ quantization levels, $0 \leqslant \theta \leqslant 1$ is divided into $(2^N - 1)$ equal-size quantization intervals of length $1/(2^N - 1)$. To ensure adaption when $\theta$ is off by one quantization interval or more, we want

$$\xi < \frac{1}{2^N - 1}.$$

Furthermore, we do not want $\theta$ to change when it is off by less than one-half of a quantization interval, so that

$$\xi > \frac{1}{2(2^N - 1)}.$$

Experimentally the value $\xi = 0.24$, which is approximately in the center of this range, proved satisfactory.

The integrator in the filter which averages $u_1$ is reset to zero for each count to prevent additional counts unless a new average shows that to be appropriate. A reset also occurs whenever the FET power (as reflected in $u_2$) falls below a threshold determined by $V_1$ or a NET is detected, thereby preventing adaptation under these conditions.

Fig. 10 illustrates how adaptation occurs for a worst case when $\theta_0 = 1$ and the actual $\theta$ starts at $\theta = 0$. The $u_1$ filter must charge and the counter must count three times before adaptation is complete. The larger $|\theta_0 - \theta|$, the faster $u_1$ reaches the threshold $\xi u_2$. In fact, for the range $0 \leqslant t \leqslant t_1$, where $t_1$ is the time of the first count, and neglecting statistical variation in $u_1$ about the mean,

$$u_1(t) \cong \sqrt{\frac{2}{\pi}}\,\sigma_w(\theta_0 - \theta)(1 - e^{-at})$$

$$u_2(t) \cong \sqrt{\frac{2}{\pi}}\,\sigma_w$$

so that

$$t_1 \cong \frac{1}{a}\ln\left(\frac{\theta_0 - \theta}{\theta_0 - \theta - \xi}\right)$$

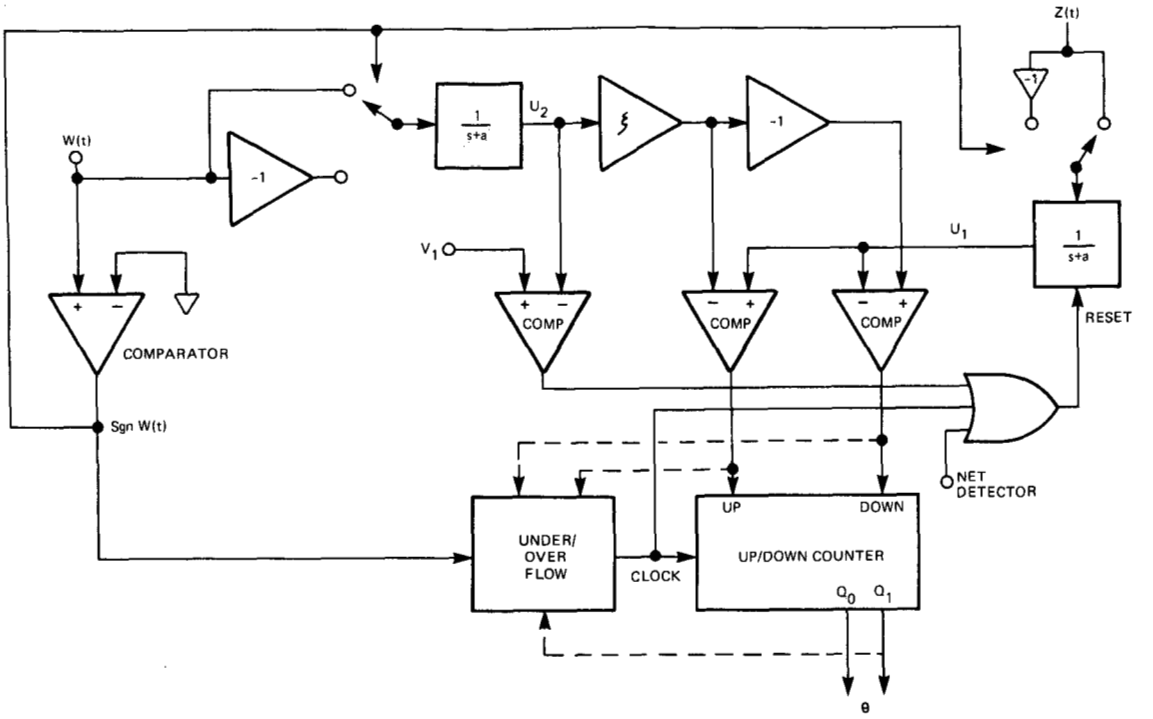


Fig. 9. Adaptation control in digital implementation.

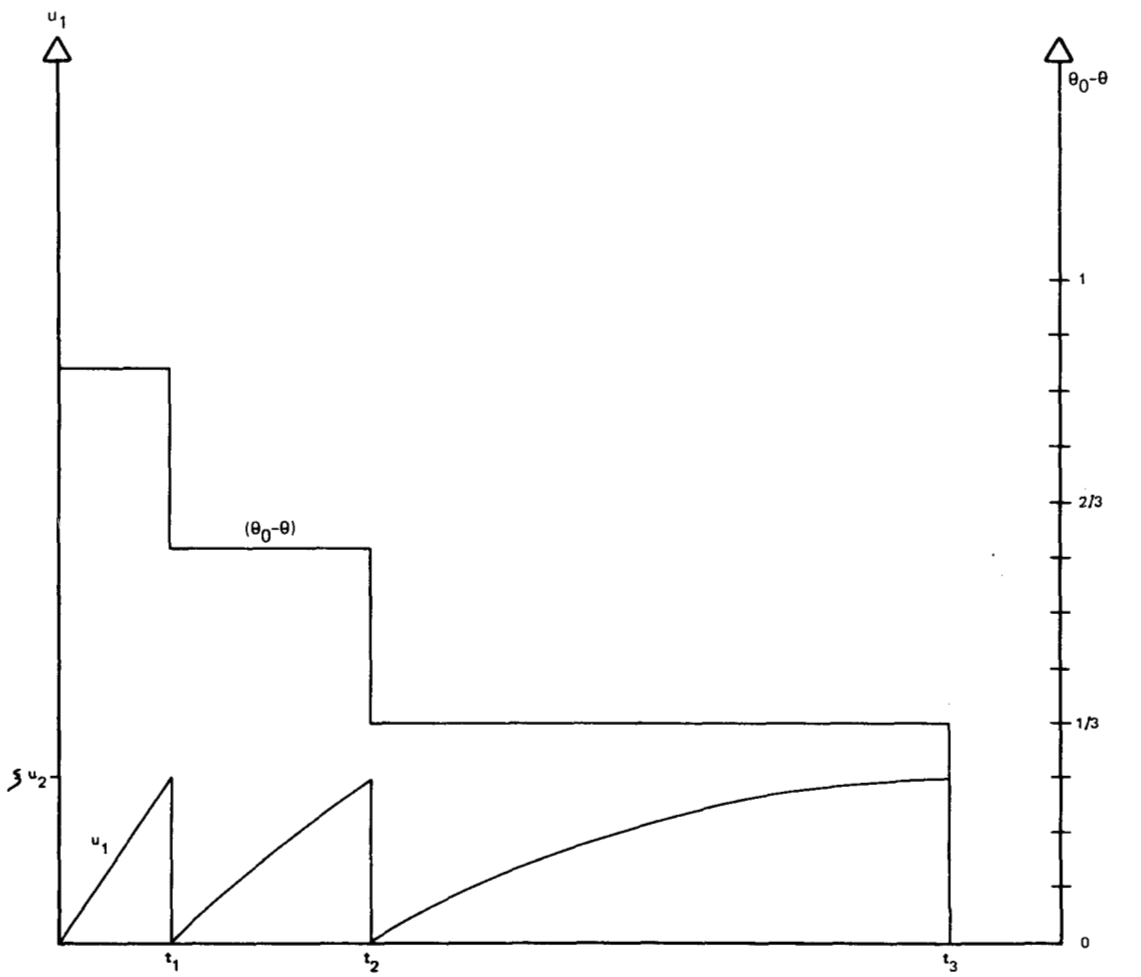


Fig. 10. Typical adaptation of digital implementation for $\theta_0 = 1$ (starting at $\theta = 0$).

decreases as $(\theta_0 - \theta)$ increases. The total worst-case adaptation time is thus

$$t_{2N-1} \cong \frac{1}{a} \sum_{i=1}^{2^N-1} \ln\left(\frac{\theta_0 - \theta_i}{\theta_0 - \theta_i - \xi}\right)$$

where $\theta_i$ is the value of $\theta$ just prior to count time $t_i$,

$$\theta_i = \frac{i-1}{2^N - 1}.$$

For the present implementation, where $\xi = 0.24$ and $a = 1\ s^{-1}$, the worst case adaptation time is $t_3 = 2.03$ s. This is confirmed in Fig. 11, where the actual $u_1(t)$ is shown, and the adaptation time is almost exactly 2 s. The primary thing to note is that through normalization of the threshold adaptation time is very insensitive to FET power, unlike the analog implementation. Of course, adaptation with a speech signal will be slower than that predicted previously due to the fact that the FET is only present a portion of the time and also due to double-talking.

Fig. 12 shows a circuit implementing the speech detector described in [1], in which the direction of flow of power is estimated. The voltage $v(t)$ (proportional to the current flowing into the loop) and the voltage $u(t)$ across the loop are each limited (by the two comparators) and cross correlated (by the EXCLUSIVE-OR and one-pole low-pass filter). The result, an estimate of

$$\rho = E\,[\operatorname{sgn} u(t) \operatorname{sgn} v(t)]$$

is compared with a threshold $\eta$, and when below that threshold is taken as an indication of a NET, so that adaptation is disabled. Experimentally $\eta = 0.3$ was chosen, and the filter time constant was 0.2 s. It was then observed using an artificial line that NET signals larger than −6 dB relative to a FET signal could be successfully detected.

The described circuit was built using standard parts, PMOS-bipolar operational amplifiers and differential comparators, and CMOS logic and analog switches. The logic was operated from the analog ±5 V supply to provide direct interfacing with the analog section.

Only one digital implementation was breadboarded, and as a result the experimental setup (shown in Fig. 13) is somewhat different than for the analog implementation. The far-end hybrid was simulated with a resistive attenuator providing a flat loss of up to 2 dB with no delay. The 8 dB gain amplifier in the receive path compensates for the hybrid loss (6 dB) and additional losses in the transformer and protection circuitry. A second amplifier in the transmit path was added to manually change the phase of the sidetone from 0 to 180° when desired. Another manual switch ($SW_5$) disables the adaptation and freezes the present state.

Experimental measurements of the adaptation time using high-level sinusoidal signals showed good match with that predicted earlier and in particular, insensitivity to signal level.

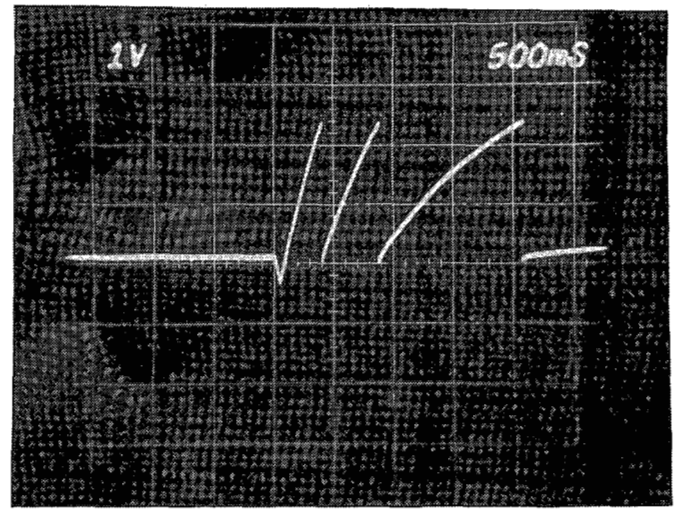


Fig. 11. $u_1$ versus time after switching from nonloaded to loaded loop (input 1 kHz sinusoid, 1 V rms).

With signal levels below −20 dBm adaptation time increased up to 3-4 s. This effect was attributed to noise and offset in the comparators. The adaptation process is inhibited for signals below −25 dBm.

With NET signal present (simulated with another generator) and the four-wire loop closed as described, some sensitivity in adaptation time was noted. The magnitude of this effect was dependent upon the phase shift imposed in the four wire loop (0-180°) and the sign of $(\theta_0 - \theta)$. Similar results were observed using noise sources (*C*-message).

Increasing the near-end interference in the absence of the NET detector up to about 4 dB below the far-end signal caused errors in the setting of $\theta$. The NET detector was, however, able to reliably disable adaptation for this large a NET signal as previously mentioned.

In operation with a voice signal source (FET alone) sporadic changes in the setting of $\theta$ were noticed, mostly associated with a change in speaker, showing the dependence of the adaptation on the power spectrum of the FET signal. This effect was only noticed with the artificial line simulating a loaded loop. Fig. 14 shows a plot of $\theta$ and the resulting trans-hybrid loss versus cable length with a *C*-message weighted noise source as the FET.

## V. CONCLUSIONS

Two implementions of an adaptive balancing hybrid have been described. The analog version, which was constructed to demonstrate feasibility, is a straightforward realization of the principles described in [1]. The digital implementation incorporates some innovations which permit indefinite retention of the last value of $\theta$, relative insensitivity to signal levels, and considerably less analog circuitry. Both circuits performed up to expectations, and in particular were able to adapt reliably even in the presence of severe double-talking. Particularly encouraging was the fact that lockup in a singing condition did not prove to be a problem.

The adaptive hybrids we have described do not appear to be

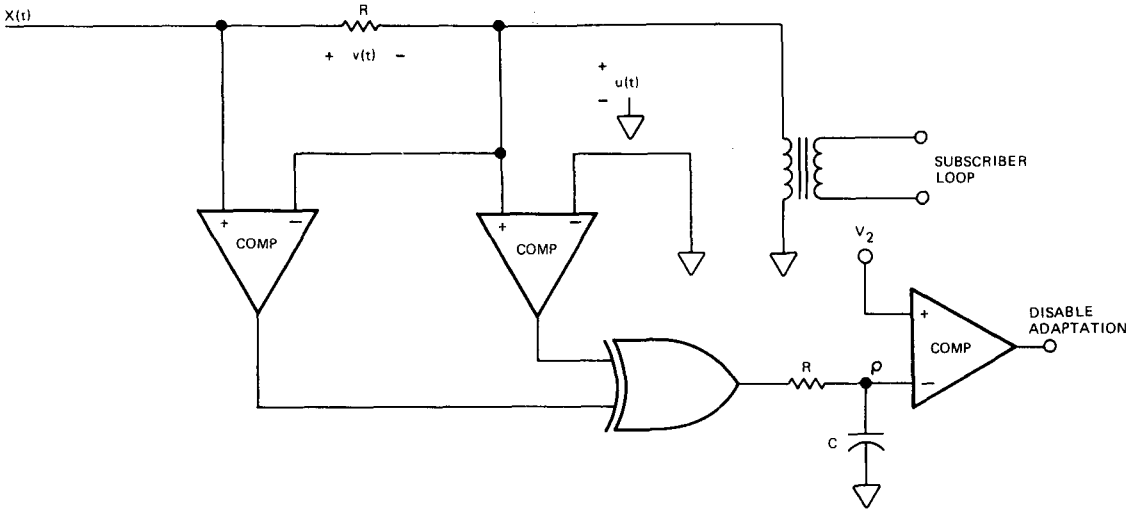


Fig. 12. NET detector in digital implementation.

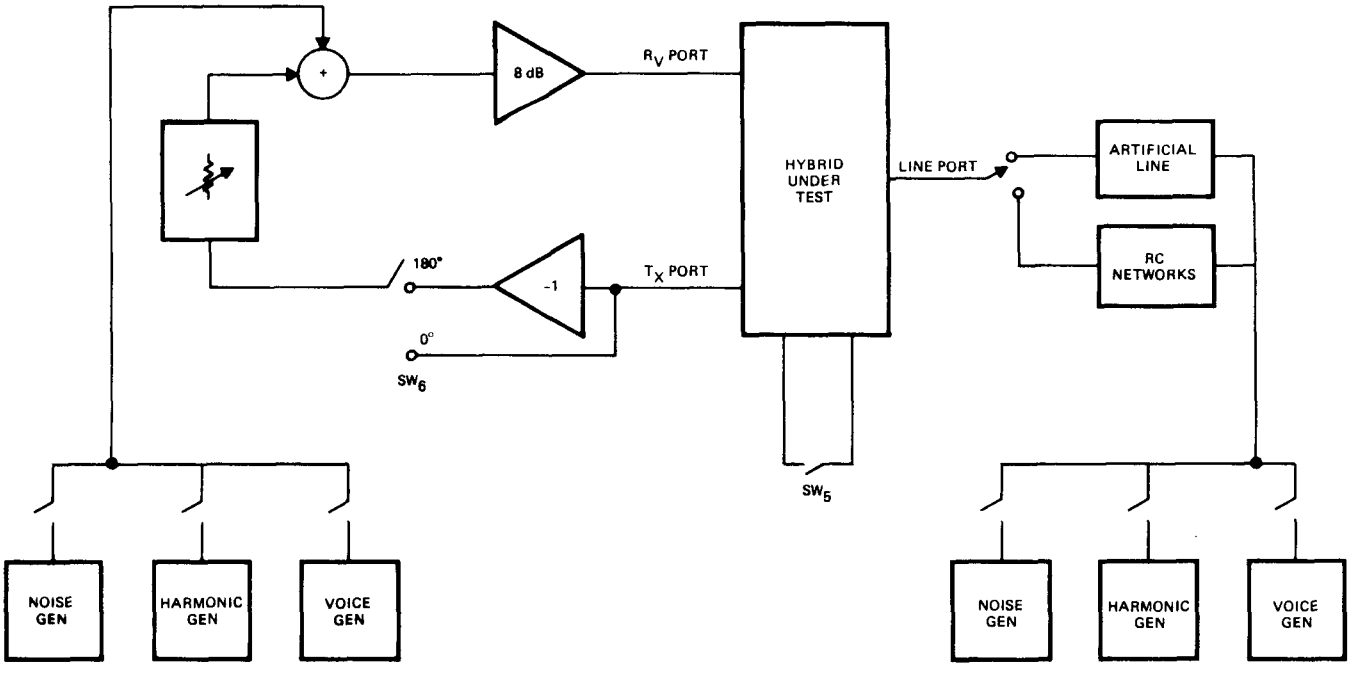


Fig. 13. Test setup for digital implementation of adaptive hybrid.

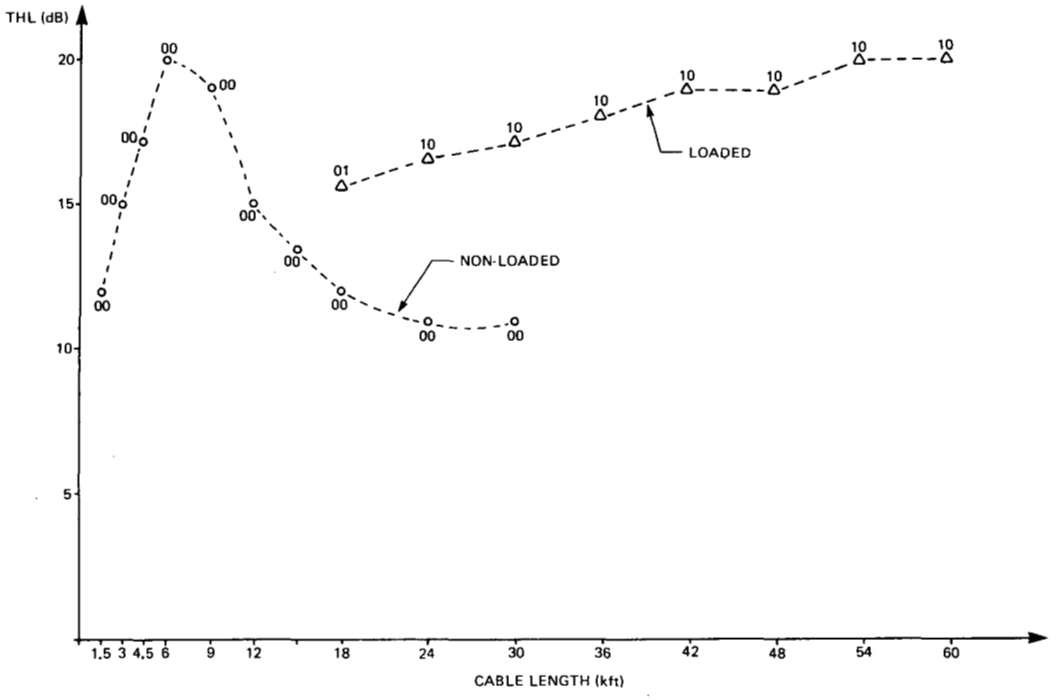


Fig. 14. Transhybrid loss and $\theta$ versus cable length.

sufficiently refined for application as yet. What is required is careful evaluation of signal levels, thresholds of adaptation, etc. Even more crucial is experience in an actual field environment, where subscriber loops can exhibit departures from ideality (such as ground leakage) which cannot be simulated by an artificial line. Another open question of a fundamental nature is the appropriate pair of terminations to use in light of the additional degree of freedom available over that provided by loop segregation alone.

## ACKNOWLEDGMENT

The authors appreciate the assistance of Mr. B. Chew in performing computer calculations and Mr. B. Todd in building the breadboard for the analog implemention.

## REFERENCES

[1] D. G. Messerschmitt, "An electronic hybrid with adaptive balancing for telephony," this issue, pp. 1399–1407.

[2] *Telecommunications Transmission Engineering*, vol. 1. Winston-Salem, NC: Western Electric Tech. Publ.

★

**Berton E. Dotter, Jr.** is a Senior Scientist at TRW VIDAR. He is currently working on system architectures for advanced digital telephone switching systems. He holds several patents on digital and analog circuit techniques for phase lock loop, timing recovery, and error detection schemes.

**Alejandro de la Plaza** was born in Mar Del Plata, Argentina, on May 29, 1947. He received the Diploma degree in electro-mechanical engineering from the University of Buenos Aires, Argentina, in 1974, and the M.S.E.E. degree from the University of California, Berkeley, in 1978.

In 1974, he joined the Institute of Biomedical Engineering of the University of Buenos Aires, where he was involved in the development and design of electronic circuits for biomedical applications. In 1978 he began the M.S. program at the University of California, where he served as a Research Assistant. Since December 1978, he has been with TRW VIDAR, in Mountain View, CA, where he is involved in the development and application of integrated circuits for telecommunications.

★

**David A. Hodges** (M'65–SM'71–F'77) received the B.E.E. from Cornell University, Ithaca, NY, and the M.S. and Ph.D. degrees in electrical engineering from the University of California, Berkeley.

From 1966 to 1970 he was at Bell Telephone Laboratories, first in the components area at Murray Hill, then as Head of the System Elements Research Department at Holmdel, NJ. He is presently Professor of Electrical Engineering and Computer Sciences at the University of California, Berkeley, where he has been a member of the faculty since 1970. He has served as a consultant in the integrated circuits and communications equipment industries. His research interests are in the area of integrated circuits and large-scale integration. He is a former Editor of the IEEE JOURNAL OF SOLID-STATE CIRCUITS (1971–1974) and has served as Program Chairman (1977) and Conference Chairman (1978) for the International Solid-State Circuits Conference.

★

**David G. Messerschmitt** (S'65–M'68–SM'78), for a photograph and biography, see this issue, p. 1407.